Alterations in nicotinic α4β2 receptor binding in vascular dementia using ^{123}I-5IA-85380 SPECT: Comparison with regional cerebral blood flow

S. J. Colloby[a*], M. J. Firbank[a], S. Pakrasi[a], E. K. Perry[a], S. L. Pimlott[b], D. J. Wyper[c], I. G. McKeith[a], E. D. Williams[d] and J. T. O'Brien[a].

[a]Institute for Ageing and Health, Newcastle University, Campus for Ageing and Vitality, Newcastle upon Tyne. NE4 5PL. UK.

[b]West of Scotland Radionuclide Dispensary, NHS Greater Glasgow and Clyde, Western Infirmary, Glasgow. UK.

[c]Department of Clinical Physics, NHS Greater Glasgow and Clyde, Southern General Hospital, Glasgow. UK.

[d]Regional Medical Physics Department, Sunderland Royal Hospital, Kayll Road, Sunderland. SR4 7TP. UK.

[*]Corresponding author:

Tel: +44 191 248 1321, e-mail: s.j.colloby@ncl.ac.uk

Abstract

Objective: To investigate differences in distribution of α4β2 subtypes of nicotinic acetylcholine receptors (nAChRs) using the ligand ^{123}I-5-Iodo-3-[2(S)-2-azetidinylmethoxy] pyridine (5IA-85380) and single photon emission computed tomography (SPECT) in subjects with vascular dementia and age-matched controls. ^{123}I-5IA-85380 binding was compared to corresponding regional cerebral blood flow (rCBF) changes in the same subjects.

*Method*s: Thirty subjects (14 vascular dementia and 16 controls) underwent ^{123}I-5IA-85380 and rCBF (^{99m}Tc-exametazime) SPECT scanning. Image analysis was performed on voxel basis using statistical parametric mapping (SPM2).

Results: Compared to controls, reductions in relative ^{123}I-5IA-85380 uptake were identified in dorsal thalamus and right caudate in vascular dementia. Increase in scaled ^{123}I-5IA-85380 uptake in cuneus was also demonstrated in vascular dementia relative to controls. Perfusion deficits in anterior cingulate were apparent in the patient group and did not appear to be associated with ^{123}I-5IA-85380 changes.

Conclusions: Reduced ^{123}I-5IA-85380 uptake in vascular dementia was confined to sub-cortical regions, unlike the cortical reductions previously described in Alzheimer's disease. Elevation of normalised ^{123}I-5IA-85380 uptake in cuneus in vascular dementia could be a compensatory response to reduced cholinergic activity in dorsal thalamus.

Keywords: SPECT; Nicotinic; Vascular dementia; SPM

1. Introduction

Nicotinic acetylcholine receptors (nAChRs) are ligand-gated cation channels whose action is controlled by acetylcholine (ACh) and nicotinic agonists. They are distributed throughout the human brain and are involved in a range of physiological processes including cognitive and sensory function, memory, learning, arousal, reward and motor control (Jones et al., 1999). The most abundant varieties of nAChRs in humans are the α4β2 and α7 subtypes (Le Novere and Changeux, 1995; Lindstrom et al., 1995). Reduction of these and other nicotinic receptor subtypes has been observed *in vitro* in Alzheimer's disease (AD), dementia with Lewy bodies (DLB) and Parkinson's disease (PD) (Court et al., 2000; Perry et al., 1994; Pimlott et al., 2004; Rinne et al., 1991; Sihver et al., 1999).

Vascular dementia (VaD), along with AD and DLB, is one of the commonest causes of dementia in older people. VaD is increasingly viewed as part of a broader spectrum of vascular cognitive impairment (O'Brien et al., 2003), and classification is largely based on the most prominent site of vascular pathology, for example multi-infarct (cortical), subcortical ischaemic and strategic-infarct (O'Brien et al., 2003). Clinical features of VaD are diverse and depend largely upon location of the vascular pathology, but impairments in attention and executive function, with slowing of motor performance and information processing are frequently seen, especially in those with subcortical VaD (O'Brien et al., 2003). In contrast, episodic memory is relatively spared, unlike AD (Babikian and Ropper, 1987).

The extent of cholinergic involvement in VaD remains controversial. Some have reported cholinergic loss (Gottfries et al., 1994; Tomimoto et al., 2005), while others found cholinergic changes only in mixed, not "pure" VaD (Perry et al., 2005). Similarly, while cholinergic replacement therapy is effective in AD and mixed dementia (Erkinjuntti et al., 2002), results from studies in VaD have generally been disappointing (Roman et al., 2005; Wilkinson et al., 2003). Few studies, all limited to autopsy, have investigated the distribution of nAChRs in VaD. Using ^{3}H-epibatidine, a ligand for the α4 nicotinic receptor, Martin-Ruiz *et al* observed significant reductions in binding in temporal cortex in VaD compared to age-matched controls. However, results were confounded by subjects having a history of tobacco smoking and when smoking histories were taken into account; α4 nAChRs did not differ amongst groups (Martin-Ruiz et al., 2000). More recently, the marker ^{125}I-5-Iodo-3-[2(S)-2-azetidinylmethoxy] pyridine (5IA-85380), a high affinity nAChR ligand that demonstrates high selectivity for the α4β2 nAChRs, has also been investigated. In autopsy studies, receptor binding in VaD was found to be indistinguishable from age-matched controls in entorhinal cortex, insula, recticular nucleus, striatum, subthalamic nucleus, substantia nigra and various thalamic nuclei (Pimlott et al., 2004), in contrast to reductions in most of these regions in AD.

Neuropathological studies of nAChRs in dementia provide important information but are limited as they are restricted to end stage disease and have to be focussed on specific brain areas. Molecular *in vivo* imaging has been shown to have a role in assessing various subunits of nAChRs in vivo in AD and DLB (Kadir et al., 2006; Nordberg et al., 1995; O'Brien et al., 2007, 2008). Presently, no imaging studies have investigated nAChRs in

antemortem VaD. Regional cerebral blood flow (rCBF) and metabolic patterns have been assessed in VaD of the sub-cortical type using functional single photon emission computed tomography (SPECT) and positron emission tomography (PET) imaging with FDG. Such patterns are generally related to the nature and location of infarcts, although hypoperfusion of anterior cingulate appears a consistent feature (Hanyu et al., 2004; Shim et al., 2006; Yang et al., 2002). Similarly, PET studies have revealed that metabolic reductions are predominantly in frontal lobe and anterior cingulate (Nagata et al., 2000; Sultzer et al., 1995), while others report more diffuse changes (Kerrouche et al., 2006).

In the present study, we investigated differences in normalised ^{123}I-5IA-85380 SPECT binding (an estimate of α4β2 nAChR status) in VaD relative to age-matched controls. In addition, we compared the difference in nicotinic pattern to the associated perfusion pattern obtained from ^{99m}Tc-exametazime SPECT scanning. In accordance with previous autopsy and rCBF SPECT evaluations, we hypothesised that in VaD (excluding sites of infarcts), relative ^{123}I-5IA-85380 uptake is preserved in temporal and sub-cortical regions but rCBF would be reduced in anterior cingulate, frontal, temporal, and sub-cortical areas. Moreover, we assumed preservation of relative ^{123}I-5IA-85380 uptake to extend to other cortical regions in VaD.

2. Methods

2.1. Subjects

The sample consisted of 14 VaD patients and 16 normal elderly control subjects (non-smoking for more than 10 years). Patients were gathered from patients who had been referred to local community stroke and old age psychiatry services. Normal controls were recruited from friends and spouses of patients included in this and other research studies. All subjects underwent ^{123}I-5IA-85380 and ^{99m}Tc-exametazime SPECT scanning. The study was approved by the local research ethics committee and UK Department of Health's Administration of Radioactive Substances Advisory Committee (ARSAC). All participants, as well as the nearest relative for patients, gave informed written consent.

2.2. Assessments and diagnosis

Participants underwent physical, neurological and neuropsychiatric examinations, which included history, mental state and physical examination, and for VaD patients, a standard blood screen with thyroid function tests, B12, folate and syphilis serology and CT brain scan. Standardised assessments included the Mini-Mental State Examination (MMSE) (Folstein et al., 1975), the Cambridge Cognitive Examination (CAMCOG) (Roth et al., 1986), the Neuropsychiatric Inventory (NPI) (Cummings et al., 1994) and fluctuation assessment scale (Walker et al., 2000). Diagnosis of VaD was made by consensus between two experienced researchers (J. T. O'Brien, S. Pakrasi) using the NINDS/ADRDA criteria for VaD (Roman, 2002). VaD patients were not receiving any cholinesterase medication. Controls had no evidence of cognitive disturbance, did not

complain of poor memory and all scored within normal range of cognitive tests (lowest CAMCOG score 91, lowest MMSE score 27).

2.3. Radiochemistry

The synthesis of ^{123}I-5IA-85380 was carried out by the West of Scotland Radionuclide Dispensary, Glasgow University, as has been previously described (O'Brien et al., 2007). The dose was calibrated to the time of injection and transported to the department of nuclear medicine on the day before use.

2.4. Image acquisition

Subjects were imaged using a triple-headed rotating gamma camera (Picker 3000XP) fitted with a high resolution fan-beam collimator, approximately 2 hours after a bolus intravenous injection of ^{123}I-5IA-85380. Scanning at 2 hours was chosen from time activity curve data and practical issues of imaging the patient group as previously described (O'Brien et al., 2007, 2008). This was the start of a period over which uptake ratio (regional uptake: whole brain uptake) in cortical regions remained relatively constant. Subsequently, one hundred and twenty 15 second views over a 360° orbit were acquired on a 128×128 matrix with a pixel and slice thickness of 3.5mm. Imaging time was 30 minutes. Images were reconstructed using ramp-filtered backprojection with a Butterworth filter (order 13, cut-off 0.3 cycles.cm^{-1}), then resampled to a 64×64 matrix containing 4.0mm cubic voxels. The reconstructed images were then corrected for gamma ray attenuation using Chang's method (μ = 0.11cm^{-1}). Approximately one month after their ^{123}I-5IA-85380 scan; all subjects, with the exception of one VaD patient,

underwent rCBF SPECT scanning 10 minutes after injection of 500 MBq of ^{99m}Tc-exametazime (Ceretec, GE Healthcare, also referred to as HMPAO). Image processing and reconstruction was as above. All imaging data were then transferred to a PC for further analysis.

2.5. Image analysis

Imaging data for both radiotracers were initially converted from DICOM to Analyze formats using MRIcro (http://www.sph.sc.edu/comd/rorden/mricro.html). Spatial pre-processing and statistical analysis of datasets were then performed using SPM2 (http://www.fil.ion.ucl.ac.uk/spm) and MATLAB 7.1 running on a PC under Windows XP. First, all image volumes were required to be spatially normalised to match a perfusion ^{99m}Tc-exametazime SPECT template in standard MNI space (Montreal Neurological Institute, http://www2.bic.mni.mcgill.ca/). One possible drawback of using the MNI standard brain is that it was generated from much younger populations than those in the present study, but given the spatial resolution of the current dataset (~ 10 mm); this was unlikely to affect the registrations. It was apparent from the scans that 10 of the 14 VaD subjects had at least one significant cortical infarct/lesion. Such infarcts could lead to suboptimal spatial normalisation as the registration algorithm attempts to reduce image mismatch between the template and image at the site of the infarct. To avoid this, we masked the infarct during the normalisation, so that the infarct did not bias the transformations (Brett et al., 2001). Therefore, each subject underwent the following spatial pre-processing:

a) Within-mode coregistration between the ^{99m}Tc-exametazime and ^{123}I-5IA-85380 scans (target image = ^{99m}Tc-exametazime, object image = ^{123}I-5IA-85380).

b) Using MRIcro, a mask image of the infarct/lesion was produced from the ^{99m}Tc-exametazime scan (if appropriate).

c) Spatial normalisation (12-parameters affine) with function masking (if appropriate) of ^{99m}Tc-exametazime scan to SPECT template in standard MNI space.

d) 3D transformation parameters calculated in (c) applied to the coregistered ^{123}I-5IA-85380 scan.

e) Spatial smoothing of registered scans using 10mm FWHM 3D Gaussian filter.

Fig. 1 illustrates an example of lesion masking for two VaD cases. Since registration accuracy was of a similar order to spatial resolution, image registration using purely linear transformations was considered satisfactory (Acton and Friston, 1998). The template image was generated from 39 elderly controls as previously described (O'Brien et al., 2007, 2008). Voxel size was preserved before and after spatial normalisation. All spatially normalised images were visually inspected to ensure accuracy of registrations.

Once the images had undergone spatial pre-processing, the general linear model was employed to perform the appropriate voxelwise statistical tests (two sample t-test) in the assessment of group differences in relative ^{123}I-5IA-85380 and ^{99m}Tc-exametazime uptake separately between VaD and controls. Correlations in VaD were investigated for each variable using linear regression with variables entered as covariates. Image intensity was normalised between subjects to prevent intersubject variability masking the regional changes. This was performed using proportional scaling (Frackowiak et al., 1997), where each image was scaled to its mean global brain activity (counts.voxel^{-1}). Grey matter

threshold was set to 0.8, as this appeared effectively to exclude infarcts, extracerebral tissue and ventricles. Group effects and linear regression were assessed using a probability height threshold of $P \leq 0.001$ uncorrected for multiple non-independent comparisons. Statistical inference was estimated from the distributional approximations from Gaussian random field theory (Friston et al., 1994). Regions were interpreted and reported as significant if their multiple-comparison corrected cluster-level significance was ≤ 0.05.

2.6. Display of results

Regions of significant difference in normalised ^{123}I-5IA-85380 and ^{99m}Tc-exametazime scans were displayed as maximum intensity projections (glass brain) in three orthogonal planes. These maps were also displayed on selected planes of the ^{99m}Tc-exametazime SPECT template. All statistical maps were displayed for height thresholds of $P_{uncorrected} \leq 0.001$, extent (k) ≥ 16 voxels (approx 1 cm^3). Result localisation was performed by transformation from MNI to Talairach space (Brett, 1999), followed by input into the Talairach Daemon (http://www.talairach.org/daemon.html).

3. Results

3.1. Subject characteristics

Table 1 shows demographic and neuropsychological characteristics of controls and VaD. Groups were matched for age ($F_{1,\ 28}$=1.6, p=0.2) and sex (χ^2=0.3, df=1, p=0.6). As expected, VaD subjects performed worse on cognitive assessments than controls, i.e., MMSE ($F_{1,\ 28}$=37.3, p<0.001), CAMCOG ($F_{1,\ 28}$=30.5, p<0.001), $CAMCOG_{memory}$ ($F_{1,\ 28}$=23.3, p<0.001) and executive function ($F_{1,\ 28}$=40.8, p<0.001). In addition, according to NPI, 2 patients were depressed, 2 had hallucinations, and one had delusions. Of these subjects, 4 were receiving psychotropic medications. The two patients with depression were taking antidepressants. Of the two with hallucinations, one was taking an antipsychotic, the other an antipsychotic as well as anticonvulsant medication.

3.2. Differences in ^{123}I-5IA-85380 and ^{99m}Tc-exametazime binding between VaD and controls

Fig. 2A shows the SPM map of decreased relative ^{123}I-5IA-85380 uptake in VaD compared to controls. Reductions were apparent in sub-cortical structures such as dorsal thalamus, right caudate and white matter. Table 2A lists the location and peak statistical measures. In addition, a significant increase in normalised ^{123}I-5IA-85380 uptake was observed in the cuneus bilaterally and in the right middle occipital gyrus in VaD relative to controls (fig. 2B), where table 2B details the location and peak statistical measures. Fig. 2C shows both results superimposed onto the ^{99m}Tc-exametazime SPECT template, illustrating the loss (blue region) and increase (orange region) of normalised ^{123}I-5IA-85380 uptake in VaD.

Changes in perfusion were investigated between VaD and controls. Marked deficits in rCBF were discovered in the anterior cingulate bilaterally in VaD compared to controls (fig. 3A and 3B). There were no regions where increases in ^{99m}Tc-exametazime binding were found in VaD relative to controls. Table 3 lists the location and peak statistical measures of the rCBF comparisons. Differences in rCBF and ^{123}I-5IA-85380 between groups revealed distinct patterns. Fig. 4 shows representative ^{123}I-5IA-85380 and ^{99m}Tc-exametazime SPECT scans axially in MNI space of a control and VaD patient, where thalamic decline and cuneal increase in ^{123}I-5IA-85380 binding was evident in VaD but not in the control, results which were quite different from perfusion changes.

3.3. Association between thalamic and cuneal ^{123}I-5IA-85380 uptake in VaD

In an attempt to understand the apparent cuneal upregulation in VaD, and because of the known strong thalamo-occipital connections (including cholinergic) (Behrens et al., 2003; Johansen-Berg et al., 2005), the relationship between thalamic and cuneal ^{123}I-5IA-85380 uptake in VaD was investigated. Normalised mean counts.voxel^{-1} for each significant cluster (figs. 2A and 2B) were extracted from scans using the SPM toolbox MarsBaR software (MARSeille Boîte À Région d'Intérêt) (Brett et al., 2002). The cluster data were then plotted (fig. 5), showing a negative trend (Pearson's correlation coefficient $r = -0.43$, $p=0.06$) between thalamus and cuneal cluster binding in VaD.

3.4. Clinical and neuropsychological correlates of ^{123}I-5IA-85380 and ^{99m}Tc-exametazime uptake in VaD

The relationship between image uptake and variables (sex, age, CAMCOG, $CAMCOG_{memory}$, executive function, fluctuation, NPI score) were investigated in VaD. No significant effects in any brain region were observed between these variables and ^{123}I-5IA-85380 and ^{99m}Tc-exametazime imaging data**.**

4. Discussion

Using SPECT we investigated normalised ^{123}I-5IA-85380 uptake, an estimate of α4β2 nAChRs, in VaD compared to aged-matched controls. Decreased uptake in VaD was confined to sub-cortical areas, the dorsal thalamus, right caudate and white matter, while cortical regions were unaffected. Results support our hypothesis of preserved nAChRs in temporal cortex in VaD and are consistent with an autopsy study which used the α4β2 affinity nicotinic ligand ^{3}H-epibatidine to demonstrate temporal preservation in VaD relative to controls (Martin-Ruiz et al., 2000). Deficits in thalamus and right caudate were more unexpected, although the thalamus has been shown to be associated with a strong age-related decline in nAChR availability (32%, 4.8% decade^{-1}) (Mitsis et al., 2008). Interestingly, Pimlott *et al*, observed an 11% reduction in ^{125}I-5IA-85380 binding in tissue of the anteroprincipal nucleus of the thalamus, a region of the dorsal thalamus, in VaD compared to controls, but this was not statistically significant (Pimlott et al., 2004): small sample size reduced statistical power in that study (controls n=6, VaD n=3).

Depletion of various nAChR subtypes in thalamus has been reported in AD and DLB at autopsy. ^{125}I-α-bungarotoxin, a ligand used to visualise α7 nAChRs, was shown to be reduced in reticular nucleus in AD and DLB (Court et al., 2001; Court et al., 1999). Using ^{3}H-nicotine, uptake was found to be lower in the lateral dorsal nucleus in DLB (Court et al., 1999), while for AD, there was an overall trend for decrease in most thalamic nuclei (Court et al., 2001). Decline of α6/α3 nAChRs in DLB has also been demonstrated in thalamus using ^{125}I-α-conotoxinMII (Ray et al., 2004), but previous ^{123}I-5IA-85380 investigations by the present authors did not reveal any significant alterations

in AD or DLB antemortem in thalamic binding. The discrepancy was most likely due to the study of different nAChR subtypes. Similarly, neuropathological and imaging studies have revealed deficits in nAChRs in striatum (caudate) in AD (O'Brien et al., 2007; Pimlott et al., 2004; Rinne et al., 1991) and to an even greater extent in DLB (O'Brien et al., 2008; Pimlott et al., 2004; Ray et al., 2004). Nicotinic cholinergic deficits in thalamus and striatum are associated with all three main subtypes of late life dementia, possibly suggesting an important role in common cognitive impairments involving these structures, such as attention, executive function or memory dysfunctions. Further studies of cholinergic changes in these regions, combined with detailed neuropsychology will be required to investigate this further.

A significant increase in normalised ^{123}I-5IA-85380 uptake was discovered in the bilateral cuneus and right middle occipital gyrus in VaD relative to controls. This result was unexpected, and since there were no similar patterns in rCBF found within this or surrounding regions, tracer kinetic factors are an unlikely explanation. Elevated scaled ^{123}I-5IA-85380 binding in cuneus has previously been demonstrated in DLB and was associated with visual hallucinations (O'Brien et al., 2008). Visual hallucinations have also been associated with VaD, but as only 14% (2/14) of the VaD subjects in this study had a recent history of visual hallucinations we could not analyse this further. Diffusion imaging has shown a rich neural connectivity between thalamus and cortex in human brain *in vivo* (Behrens et al., 2003; Johansen-Berg et al., 2005), in particular, using a probabilistic tractography method to create a 'thalamic connectivity atlas (http://www.fmrib.ox.ac.uk/connect/)', which calculates the probability of anatomical

neural connectivity between a specific thalamic coordinate and cortex (Johansen-Berg et al., 2005). Using the atlas, peak loss of nicotinic binding in thalamus in VaD, i.e., 8 -12 20, demonstrated highest probabilities of connectivity in temporal and occipital cortices. Therefore as an exploratory exercise, the relationship between thalamic and cuneal normalised ^{123}I-5IA-85380 uptake was investigated in an attempt to understand cuneal upregulation in VaD and its possible association with uptake in thalamus. A negative trend ($p=0.06$) was observed between thalamic and cuneal cluster ^{123}I-5IA-85380 binding in VaD, which could suggest that the increase in relative ^{123}I-5IA-85380 uptake in cuneus could be a compensatory response to reduced cholinergic activity in dorsal thalamus, though this remains speculative.

Relative ^{123}I-5IA-85380 uptake in VaD showed a pattern distinct from rCBF. Significant hypoperfusion was observed in anterior cingulate in VaD compared to controls. This was broadly in agreement with previous rCBF investigations of subcortical VaD where deficits in anterior cingulate are a prominent feature (Hanyu et al., 2004; Shim et al., 2006; Yang et al., 2002). Other regions shown to be affected are frontal (Hanyu et al., 2004; Yoshikawa et al., 2003), thalamus, striatal and temporal lobes (Shim et al., 2006; Yang et al., 2002). Generally blood flow abnormalities in VaD are largely anterior. PET studies have also revealed metabolic reductions in frontal and anterior cingulate (Nagata et al., 2000; Sultzer et al., 1995). Deviation between these studies and present results are probably due to variance of VaD populations and differences in analysis methods, e.g., the use of image masking to avoid infarcts in areas of temporal and frontal lobes. As a

matter of interest, when SPM height thresholds were lowered from $P_{uncorrected} \leq 0.001$ to $P_{uncorrected} \leq 0.01$, rCBF loss extended to frontal regions.

There was no concordance between cognitive variables in VaD with relative ^{123}I-5IA-85380 uptake. The lack of correlates with ^{123}I-5IA-85380 uptake has also been demonstrated in previous studies with AD and DLB and also with non-demented PD subjects (Fujita et al., 2006; O'Brien et al., 2007, 2008). Results may have been due to the small sample size, rudimentary nature of the cognitive measures, significant α4β2 receptor loss occurring early before symptoms, or lack of sensitivity of nicotinic SPECT data to cognitive changes.

Limitations of the present study included small sample size and in analysis methodology of which has been explained in a previous report, i.e., scaling the imaging data to mean global brain activity (O'Brien et al., 2008). The current method does not give an absolute quantitative measure of α4β2 nAChRs and cannot detect global changes. Absolute quantification of nAChRs requires either information via plasma tracer measurements or selection of a suitable reference region without nAChRs. Blood sampling was not practical for our VaD population, and no brain area devoid of nAChRs has been described. In addition, an age related decline in nicotinic ^{123}I-5IA-85380 SPECT binding has been demonstrated (Mitsis et al. 2008), and due to lack of evidence, the effect of gender on ^{123}I-5IA-85380 uptake is unclear. In our study both age and gender were (i) balanced across groups and (ii) did not significantly correlate with the imaging data. Hence for the main analyses, we did not control for these variables.

In conclusion, this was the first study to examine the distribution of relative in ^{123}I-5IA-85380 uptake *in vivo* in VaD using SPM2. The measurement of ^{123}I-5IA-85380 may be affected by differences in rCBF between groups but the results indicated that such possibilities are small. Compared to controls, significant reductions in normalised ^{123}I-5IA-85380 uptake were confined to sub-cortical regions (principally dorsal thalamus) in VaD, whereas in cortical regions in accordance with previous studies, uptake was preserved. Unexpectedly, significant elevation of normalised ^{123}I-5IA-85380 uptake was observed in cuneus in VaD relative to controls and could be a compensatory response to reduced cholinergic activity in dorsal thalamus. The ^{123}I-5IA-85380 results in VaD are merely suggestive and therefore require further independent verification.

Acknowledgements

We thank the Alzheimer's Society for financial support. We thank staff at the Regional Medical Physics Department, Nuclear Medicine Section, Newcastle General Hospital and all members of the clinical research team who helped with patient recruitment. The authors report no conflicts of interest.

References

Acton, P.D., Friston, K.J., 1998. Statistical parametric mapping in functional neuroimaging: beyond PET and fMRI activation studies. Eur. J. Nucl. Med. Mol. Imaging. 25 (7), 663-667.

Babikian, V., Ropper, A.H., 1987. Binswanger's disease: a review. Stroke. 18 (1), 2-12.

Behrens, T.E., Johansen-Berg, H., Woolrich, M.W., Smith, S.M., Wheeler-Kingshott, C.A., Boulby, P.A., Barker, G.J., Sillery, E.L., Sheehan, K., Ciccarelli, O., Thompson, A.J., Brady, J.M., Matthews, P.M., 2003. Non-invasive mapping of connections between human thalamus and cortex using diffusion imaging. Nat. Neurosci. 6 (7), 750-757.

Brett, M., 1999. The MNI brain and the Talairach Atlas. MRC Cognition and Brain Sciences Unit. http://www.mrc-cbu.cam.ac.uk/Imaging/contents.html.

Brett, M., Anton, J.-L., Valabregue, R., Poline, J.B., 2002. Region of interest analysis using an SPM toolbox. Neuroimage. 6 (2).

Brett, M., Leff, A.P., Rorden, C., Ashburner, J., 2001. Spatial normalization of brain images with focal lesions using cost function masking. Neuroimage. 14 (2), 486-500.

Court, J., Martin-Ruiz, C., Piggott, M., Spurden, D., Griffiths, M., Perry, E., 2001. Nicotinic receptor abnormalities in Alzheimer's disease. Biol. Psychiatry. 49 (3), 175-184.

Court, J., Spurden, D., Lloyd, S., McKeith, I., Ballard, C., Cairns, N., Kerwin, R., Perry, R., Perry, E., 1999. Neuronal nicotinic receptors in dementia with Lewy bodies and schizophrenia: alpha-bungarotoxin and nicotine binding in the thalamus. J. Neurochem. 73 (4), 1590-1597.

Court, J.A., Piggott, M.A., Lloyd, S., Cookson, N., Ballard, C.G., McKeith, I.G., Perry, R.H., Perry, E.K., 2000. Nicotine binding in human striatum: elevation in schizophrenia and reductions in dementia with Lewy bodies, Parkinson's disease and Alzheimer's disease and in relation to neuroleptic medication. Neuroscience. 98 (1), 79-87.

Cummings, J.L., Mega, M., Gray, K., Rosenberg-Thompson, S., Carusi, D.A., Gornbein, J., 1994. The Neuropsychiatric Inventory: comprehensive assessment of psychopathology in dementia. Neurology. 44 (12), 2308-2314.

Erkinjuntti, T., Kurz, A., Gauthier, S., Bullock, R., Lilienfeld, S., Damaraju, C.V., 2002. Efficacy of galantamine in probable vascular dementia and Alzheimer's disease combined with cerebrovascular disease: a randomised trial. Lancet. 359 (9314), 1283-1290.

Folstein, M.F., Folstein, S.E., McHugh, P.R., 1975. "Mini-mental state". A practical method for grading the cognitive state of patients for the clinician. J. Psychiatric. Res. 12 (3), 189-198.

Frackowiak, R.S., Friston, K.J., Frith, C.D., Dolan, R.J., Mazziotta, J.C., 1997. Human Brain Function, First ed. Academic Press, London.

Friston, K.J., Worsley, K.J., Frackowiak, R.S.J., Mazziotta, J.C., Evans, A.C., 1994. Assessing the significance of focal activations using their spatial extent. Hum. Brain. Map. 1 (1), 214-220.

Fujita, M., Ichise, M., Zoghbi, S.S., Liow, J.S., Ghose, S., Vines, D.C., Sangare, J., Lu, J.Q., Cropley, V.L., Iida, H., Kim, K.M., Cohen, R.M., Bara-Jimenez, W., Ravina, B., Innis, R.B., 2006. Widespread decrease of nicotinic acetylcholine receptors in Parkinson's disease. Ann. Neurol. 59 (1), 174-177.

Gottfries, C.G., Blennow, K., Karlsson, I., Wallin, A., 1994. The neurochemistry of vascular dementia. Dementia. 5 (3-4), 163-167.

Hanyu, H., Shimuzu, S., Tanaka, Y., Takasaki, M., Koizumi, K., Abe, K., 2004. Cerebral blood flow patterns in Binswanger's disease: a SPECT study using three-dimensional stereotactic surface projections. J. Neurol. Sci. 220 (1-2), 79-84.

Johansen-Berg, H., Behrens, T.E., Sillery, E., Ciccarelli, O., Thompson, A.J., Smith, S.M., Matthews, P.M., 2005. Functional-anatomical validation and individual variation of diffusion tractography-based segmentation of the human thalamus. Cereb. Cortex. 15 (1), 31-39.

Jones, S., Sudweeks, S., Yakel, J.L., 1999. Nicotinic receptors in the brain: correlating physiology with function. Trends. Neurosci. 22 (12), 555-561.

Kadir, A., Almkvist, O., Wall, A., Langstrom, B., Nordberg, A., 2006. PET imaging of cortical (11)C-nicotine binding correlates with the cognitive function of attention in Alzheimer's disease. Psychopharmacology (Berl). 188 (4), 509-520.

Kerrouche, N., Herholz, K., Mielke, R., Holthoff, V., Baron, J.C., 2006. 18FDG PET in vascular dementia: differentiation from Alzheimer's disease using voxel-based multivariate analysis. J. Cereb. Blood. Flow. Metab. 26 (9), 1213-1221.

Le Novere, N., Changeux, J.P., 1995. Molecular evolution of the nicotinic acetylcholine receptor: an example of multigene family in excitable cells. J. Mol. Evol. 40 (2), 155-172.

Lindstrom, J., Anand, R., Peng, X., Gerzanich, V., Wang, F., Li, Y., 1995. Neuronal nicotinic receptor subtypes. Ann. N Y. Acad. Sci. 757, 100-116.

Martin-Ruiz, C., Court, J., Lee, M., Piggott, M., Johnson, M., Ballard, C., Kalaria, R., Perry, R., Perry, E., 2000. Nicotinic receptors in dementia of Alzheimer, Lewy body and vascular types. Acta. Neurol. Scand. Suppl. 176, 34-41.

Mitsis, E.M., Cosgrove, K.P., Staley, J.K., Bois, F., Frohlich, E.B., Tamagnan, G.D., Estok, K.M., Seibyl, J.P., van Dyck, C.H., 2008. Age-related decline in nicotinic receptor availability with [(123)I]5-IA-85380 SPECT. Neurobiol. Aging.

Nagata, K., Maruya, H., Yuya, H., Terashi, H., Mito, Y., Kato, H., Sato, M., Satoh, Y., Watahiki, Y., Hirata, Y., Yokoyama, E., Hatazawa, J., 2000. Can PET data differentiate Alzheimer's disease from vascular dementia? Ann. N Y. Acad. Sci. 903, 252-261.

Nordberg, A., Lundqvist, H., Hartvig, P., Lilja, A., Langstrom, B., 1995. Kinetic analysis of regional (S)(-)11C-nicotine binding in normal and Alzheimer brains--in vivo assessment using positron emission tomography. Alzheimer. Dis. Assoc. Disord. 9 (1), 21-27.

O'Brien, J.T., Colloby, S.J., Pakrasi, S., Perry, E.K., Pimlott, S.L., Wyper, D.J., McKeith, I.G., Williams, E.D., 2007. Alpha4beta2 nicotinic receptor status in Alzheimer's disease using 123I-5IA-85380 single-photon-emission computed tomography. J. Neurol. Neurosurg. Psychiatry. 78 (4), 356-362.

O'Brien, J.T., Colloby, S.J., Pakrasi, S., Perry, E.K., Pimlott, S.L., Wyper, D.J., McKeith, I.G., Williams, E.D., 2008. Nicotinic alpha4beta2 receptor binding in dementia with Lewy bodies using (123)I-5IA-85380 SPECT demonstrates a link between occipital changes and visual hallucinations. Neuroimage. 40 (3), 1056-1063.

O'Brien, J.T., Erkinjuntti, T., Reisberg, B., Roman, G., Sawada, T., Pantoni, L., Bowler, J.V., Ballard, C., DeCarli, C., Gorelick, P.B., Rockwood, K., Burns, A., Gauthier, S., DeKosky, S.T., 2003. Vascular cognitive impairment. Lancet. Neurol. 2 (2), 89-98.

Perry, E., Ziabreva, I., Perry, R., Aarsland, D., Ballard, C., 2005. Absence of cholinergic deficits in "pure" vascular dementia. Neurology. 64 (1), 132-133.

Perry, E.K., Haroutunian, V., Davis, K.L., Levy, R., Lantos, P., Eagger, S., Honavar, M., Dean, A., Griffiths, M., McKeith, I.G., al., e., 1994. Neocortical cholinergic activities differentiate Lewy body dementia from classical Alzheimer's disease. Neuroreport. 5 (7), 747-749.

Pimlott, S.L., Piggott, M., Owens, J., Greally, E., Court, J.A., Jaros, E., Perry, R.H., Perry, E.K., Wyper, D., 2004. Nicotinic acetylcholine receptor distribution in Alzheimer's disease, dementia with Lewy bodies, Parkinson's disease, and vascular dementia: in vitro binding study using 5-[(125)i]-a-85380. Neuropsychopharmacology. 29 (1), 108-116.

Ray, M., Bohr, I., McIntosh, J.M., Ballard, C., McKeith, I., Chalon, S., Guilloteau, D., Perry, R., Perry, E., Court, J.A., Piggott, M., 2004. Involvement of alpha6/alpha3 neuronal nicotinic acetylcholine receptors in neuropsychiatric features of Dementia with Lewy bodies: [(125)I]-alpha-conotoxin MII binding in the thalamus and striatum. Neurosci. Lett. 372 (3), 220-225.

Rinne, J.O., Myllykyla, T., Lonnberg, P., Marjamaki, P., 1991. A postmortem study of brain nicotinic receptors in Parkinson's and Alzheimer's disease. Brain. Res. 547 (1), 167-170.

Roman, G.C., 2002. Defining dementia: clinical criteria for the diagnosis of vascular dementia. Acta. Neurol. Scand. Suppl. 178, 6-9.

Roman, G.C., Wilkinson, D.G., Doody, R.S., Black, S.E., Salloway, S.P., Schindler, R.J., 2005. Donepezil in vascular dementia: combined analysis of two large-scale clinical trials. Dement. Geriatr. Cogn. Disord. 20 (6), 338-344.

Roth, M., Tym, E., Mountjoy, C.Q., Huppert, F.A., Hendrie, H., Verma, S., Goddard, R., 1986. CAMDEX A Standardised Instrument for the Diagnosis of Mental Disorder in the Elderly with Special Reference to the Early Detection of Dementia. Br. J. Psychiatry. 149, 698-709.

Shim, Y.S., Yang, D.W., Kim, B.S., Shon, Y.M., Chung, Y.A., 2006. Comparison of regional cerebral blood flow in two subsets of subcortical ischemic vascular dementia: statistical parametric mapping analysis of SPECT. J. Neurol. Sci. 250 (1-2), 85-91.

Sihver, W., Gillberg, P.G., Svensson, A.L., Nordberg, A., 1999. Autoradiographic comparison of [3H](-)nicotine, [3H]cytisine and [3H]epibatidine binding in relation to vesicular acetylcholine transport sites in the temporal cortex in Alzheimer's disease. Neuroscience. 94 (3), 685-696.

Sultzer, D.L., Mahler, M.E., Cummings, J.L., Van Gorp, W.G., Hinkin, C.H., Brown, C., 1995. Cortical abnormalities associated with subcortical lesions in vascular dementia. Clinical and position emission tomographic findings. Arch. Neurol. 52 (8), 773-780.

Tomimoto, H., Ohtani, R., Shibata, M., Nakamura, N., Ihara, M., 2005. Loss of cholinergic pathways in vascular dementia of the Binswanger type. Dement. Geriatr. Cogn. Disord. 19 (5-6), 282-288.

Walker, M.P., Ayre, G.A., Cummings, J.L., Wesnes, K., McKeith, I.G., O'Brien, J.T., Ballard, C.G., 2000. The Clinician Assessment of Fluctuation and the One Day Fluctuation Assessment Scale. Two methods to assess fluctuating confusion in dementia. Br. J. Psychiatry. 177, 252-256.

Wilkinson, D., Doody, R., Helme, R., Taubman, K., Mintzer, J., Kertesz, A., Pratt, R.D., 2003. Donepezil in vascular dementia: a randomized, placebo-controlled study. Neurology. 61 (4), 479-486.

Yang, D.W., Kim, B.S., Park, J.K., Kim, S.Y., Kim, E.N., Sohn, H.S., 2002. Analysis of cerebral blood flow of subcortical vascular dementia with single photon emission computed tomography: adaptation of statistical parametric mapping. J. Neurol. Sci. 203-204, 199-205.

Yoshikawa, T., Murase, K., Oku, N., Kitagawa, K., Imaizumi, M., Takasawa, M., Nishikawa, T., Matsumoto, M., Hatazawa, J., Hori, M., 2003. Statistical image analysis of cerebral blood flow in vascular dementia with small-vessel disease. J. Nucl. Med. 44 (4), 505-511.

Table 1

Demographic and neuropsychological data of subjects studied with ^{123}I-5IA-85380 and ^{99m}Tc-exametazime SPECT.

	Control	**VaD**	**p value**
n	16	14	
Sex (M: F)	10: 6	10: 4	Ns
Age	75.4 ± 4.5	77.7 ± 5.5	Ns
MMSE (max 30)	28.8 ± 1.1	20.7 ± 5.2	<0.001
CAMCOG (max 107)	97.9 ± 3.8	69.9 ± 19.9	<0.001
$CAMCOG_{memory}$ (max 27)	24.0 ± 1.8	15.9 ± 6.4	<0.001
Executive Function (max 28)	23.3 ± 3.1	12.8 ± 5.7	<0.001
Fluctuation (max 16)	0	3.2 ± 4.3	Na
NPI_{total} (max 144)	0	10.4 ± 9.6	Na
NPI Hallucinations (Yes: No)	0: 16	2: 12	Na
NPI Delusions (Yes: No)	0: 16	1: 13	Na
NPI Depression (Yes: No)	0: 16	2: 12	Na

Values expressed as (Mean ± 1 Standard deviation)
VaD = Vascular Dementia; MMSE = Mini-Mental State Examination; CAMCOG = Cambridge Cognitive Examination; NPI = Neuropsychiatric Inventory; Ns = Not significant; Na = Not applicable.

Table 2

Location and peak significance of ^{123}I-5IA-85380 comparisons. For each peak, table shows cluster-level significance ($P_{corrected}$), spatial extent (k), t and Z scores and peak MNI coordinates together with their location and corresponding nearest Brodmann areas.

Cluster-level ($P_{corrected}$)	Extent (k)	t, Z	MNI Coordinates (x,y,z) (mm)	Anatomical Region	Brodmann Area
A (Controls > VaD)					
0.002	190	5.2, 4.3	8, -12, 20	Right thalamus, anterior nucleus	
		4.9, 4.2	4, -8, 16	Right thalamus	
		4.8, 4.1	-24, -24, 20	Left cerebrum, white matter	
		3.6, 3.2	16, 20, 12	Right caudate	
B (VaD > Controls)					
0.011	127	5.2, 4.3	0, -84, 16	Left occipital lobe, cuneus	18
		4.7, 4.0	12, -76, 32	Right occipital lobe, cuneus	7
		4.1, 3.6	12, -92, 8	Right middle occipital gyrus	18

Table 3

Location and peak significance of ^{99m}Tc-exametazime comparisons.

Cluster-level ($P_{corrected}$)	Extent (k)	t, Z	MNI Coordinates (x,y,z) (mm)	Anatomical Region	Brodmann Area
A (Controls > VaD)					
0.001	144	4.5, 3.8	-12, 20, 24	Left anterior cingulate	32
		4.4, 3.8	4, 28, 16	Right anterior cingulate	24
		3.9, 3.5	16, 0, 40	Right cingulate gyrus	24
B (VaD > Controls)					
No suprathreshold or significant clusters					

Fig. 1. Examples of lesion masking. (A) Transverse ^{99m}Tc-exametazime (perfusion) scans showing a focal infarct of the left pre and post central gyrus (VaD 1), the other (VaD 2) with widespread cortical infarcts in gyri of the right hemisphere (middle temporal, superior temporal and inferior frontal) and left hemisphere (middle occipital and middle temporal). (B) ^{99m}Tc-exametazime scans with mask (green). (C) Associated ^{123}I-5IA-85380 (nicotinic) scans.

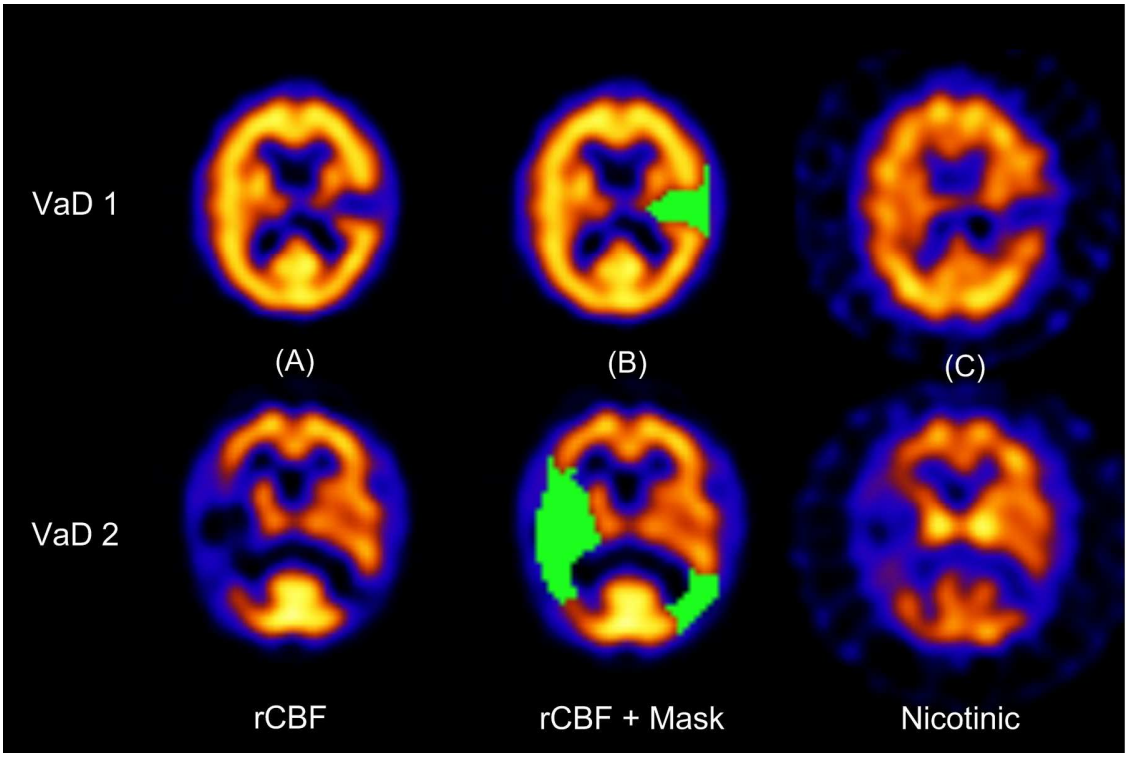

Fig. 2. SPM results ($P_{uncorrected} \leq 0.001$, $k \geq 16$ voxels) presented on a "glass brain" in the sagittal, coronal and transverse views. (A) Significant reduction of ^{123}I-5IA-85380 uptake in 14 VaD patients relative to 16 controls. (B) Significant increase in VaD compared to controls. (C) Results from (A) projected onto the ^{99m}Tc-exametazime SPECT template (blue regions) together with results from (B) (orange regions). Images presented in the neurological convention, i.e. subjects left are on left side.

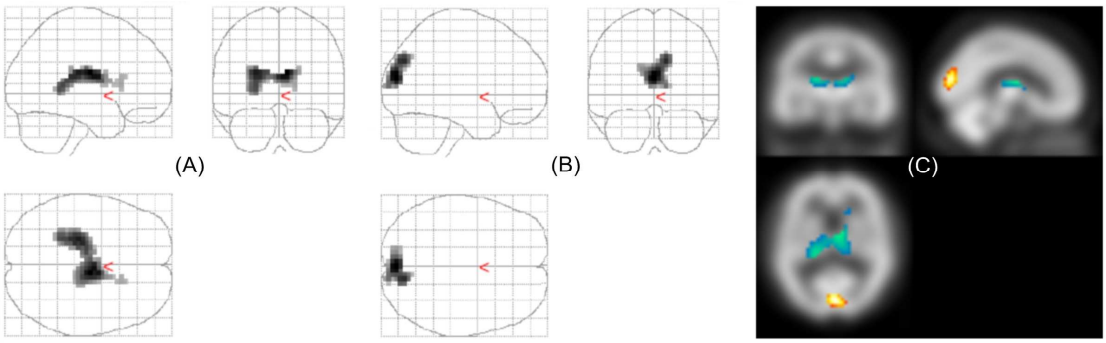

Fig. 3. SPM results ($P_{uncorrected} \leq 0.001$, $k \geq 16$ voxels) presented on a "glass brain" in the sagittal, coronal and transverse views. (A) Significant loss of ^{99m}Tc-exametazime uptake in VaD relative to controls. (B) Results from (A) projected onto the ^{99m}Tc-exametazime SPECT template (yellow region). Images presented in the neurological convention.

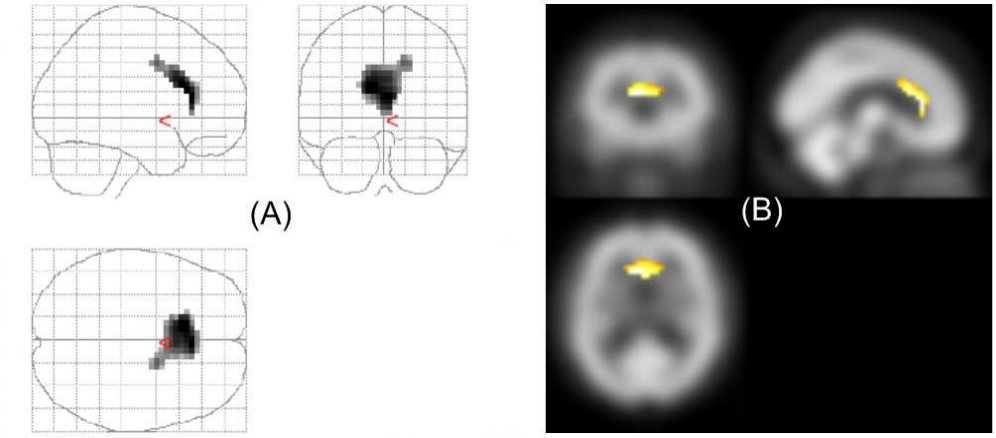

Fig. 4. Representative transverse ^{123}I-5IA-85380 and ^{99m}Tc-exametazime SPECT scans in standard MNI space of an individual control and VaD patient (matched for age and gender). Note the thalamic decline (white arrows) and cuneal increase (green arrows) in ^{123}I-5IA-85380 binding in VaD relative to the control.

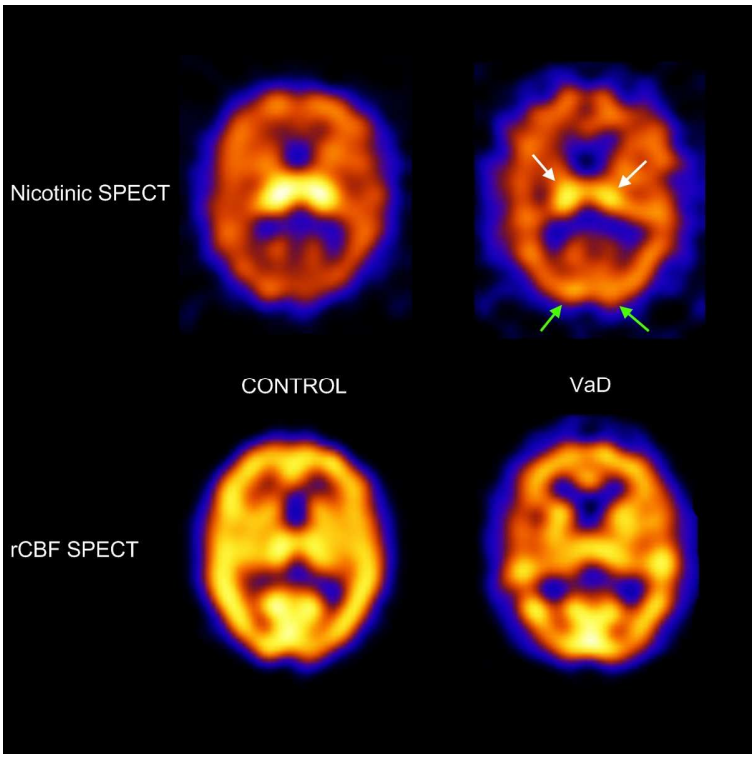

Fig. 5. Relationship between ^{123}I-5IA-85380 normalised uptake values in thalamus and in cuneal clusters in VaD subjects.